한국기계가공학회지, 제19권, 제1호, pp.81～88(2020.01) ISSN 1598-6721(Print)
Journal of the Korean Society of Manufacturing Process Engineers, Vol. 19, No. 1, pp.81~88(2020.01) ISSN 2288-0771(Online)

https://doi.org/10.14775/ksmpe.2020.19.01.081

Manufacturing Experiments using FDM 3D-printed Flexible Resistance Sensors with Heterogeneous Polymer Material Annealing

Sun Kon Lee*, Young Chan Oh, Joo Hyung Kim*,#
*Department of Mechanical Engineering, Inha University

이종 폴리머재료 어닐링을 이용한 유연저항센서 FDM 3D프린팅 제작실험

이선곤*, 오영찬*, 김주형*,#
*인하대학교 기계공학과

(Received 4 September 2019; received in revised form 17 November 2019; accepted 4 December 2019)

ABSTRACT

In this paper, the performances of the electrical characteristics of the Fused Deposition Modeling (FDM) 3D-printed flexible resistance sensor was evaluated. The FDM 3D printing flexible resistive sensor is composed of flexible-material thermoplastic polyurethane and a conductive PLA (carbon black conductive polylactic acid) polymer. While 3D printing, polymer filaments heat up quickly before being extruded and cooled down quickly. Polymers have poor thermal conductivity so the heating and cooling causes unevenness, which then results in internal stress on the printed parts due to the rapidity of the heating and cooling. Electrical resistance measurements show that the 3D-printed flexible sensor is unstable due to internal stress, so the 3D-printed flexible sensor resistance curve does not match the increases and decreases in the displacement curve. Therefore, annealing was performed to eliminate the mismatch between electrical resistance and displacement. Annealing eliminates residual stress on the sensor, so the electrical resistance of the sensor increases and decreases in proportion to displacement. Additionally, the resistance is lowered in comparison to before annealing. The results of this study will be very useful for the fabrication of various devices that employ 3D-printed flexible sensor that have multiple degrees of freedom and are not limited by size and shape.

Key Words : Additive Manufacturing(적층가공), Conductive 3D Printing(전도성 3D프린팅), 3D printing flexible resistance sensor(3D프린팅 유연저항센서), 3D printing Annealing(3D 프린팅 어닐링)

1. Introduction

A number of studies on flexible and wearable electronic devices have recently been performed. In order to implement those devices, a technique for producing thin, lightweight, and flexible devices is

Corresponding Author : sun@inha.ac.kr
Tel: +82-32-860-7320, Fax: +82-32-868-6430

needed. The device should be sufficiently flexible to take on various shapes and the device performance should be maintained even in the freely flexible condition.

As materials for producing these devices, polymers with high degrees of freedom (DOF) with respect to deformation and flexibility, such as polyimide, polydimethylsiloxane, and polyethylene terephthalate, have been used[1-2]. These existing materials should withstand various production processes that are difficult in terms of flexible device implementation and have the disadvantage that the device shape cannot be freely implemented. Hence, the study aims to produce a flexible resistance sensor (FRS) along with numerous other flexible devices using the fused deposition modeling (FDM) three-dimensional (3D) printing technique which affords a simple production process. The characteristics of the obtained sensor will also be evaluated.

The dual nozzle FDM 3D printer used to produce the FRS is a popular and widely available model with the ability to use a range of materials. It is designed to produce 3D shapes using an iterative lamination process via the high-temperature press-out extrusion of polymer filaments made from various materials[3-6]. In the present study, the 3D printed FRS was produced using thermoplastic polyurethane (TPU) to provide flexibility along with the conductive poly lactic acid (PLA). In order to optimize the process and enhance the electrical conductance of the 3D printed sensor, studies were also performed on the changes in electric resistance with increasing and decreasing displacement of the sensor before and after heat treatment (annealing). This study is expected to contribute to the expansion of FDM 3D printing into the electric and electronic application fields such as wearable and flexible devices.

2. Experiment and discussion

In this study, Proto-pasta conductive PLA was used as a printing electrode. This is a compound of NatureWorks® 4043D PLA, a dispersant, and conductive carbon black. It is characterized by vulnerability to damage because its low elasticity and brittle characteristics render it unable to provide a restoring force against external change. To overcome this problem, the flexibility of the printing sensor was ensured by providing the printing electrode with a support made of TPU, which is a flexible material with an excellent elasticity force (Fig. 1). The concept of conductive 3D printing is shown in Fig. 2.

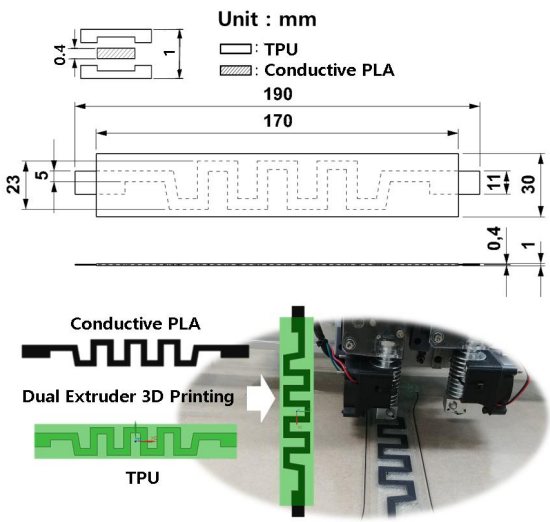

Fig. 1 Fabrication of flexible sensor using dual 3D printer

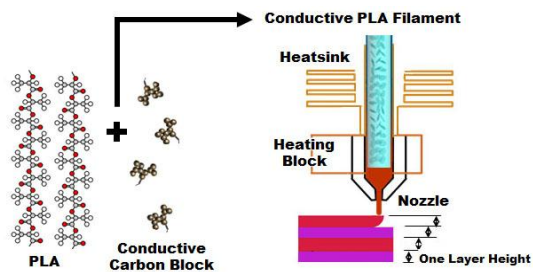

Fig. 2 Simplified schematics depicting the process of conductive PLA-based 3D printing using the technique of FDM[8]

To measure the electrical conductance according to the changing displacement of the 3D printing FRS, both ends of the sensor were fixed using a single axis actuator and the change in electric resistance was measured in real-time using a digital multimeter (34410a. Agilent) with 10 iterations of 15, 20, and 25% increase and returning-back in displacement. In addition, the change in electrical characteristics was measured using the same method after annealing the 3D printing sensor in a constant temperature oven in order to provide a comparative analysis of the characteristics before and after annealing.

To determine the annealing temperature for the FRS, the glass transition temperature (Tg) and crystallization temperature of the conductive PLA filament were measured using a differential scanning calorimeter (DSC 200F3, NETZSCH). The results of these measurements are presented in Fig. 3, in which

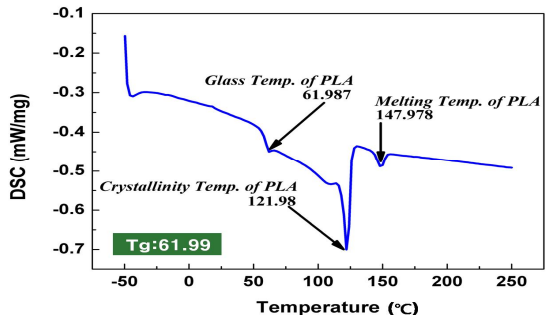

(a) PLA

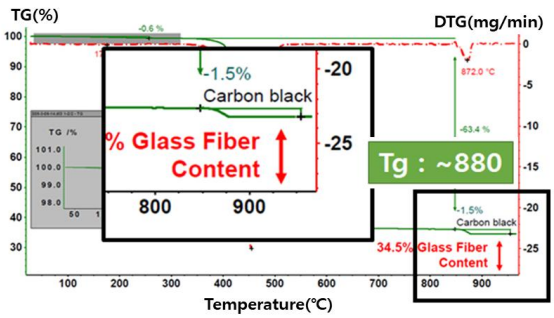

(b) Carbon black

Fig. 3 Glass transition temperature of conductive PLA Filament[8]

the Tg values of the PLA and carbon black are approximately 62 ℃ and 880 ℃, and the crystallization temperature of the PLA is approximately 120℃. Hence, the annealing temperature was set to 120 ℃ to match the crystallization temperature of the PLA.

The filament was restructured with large crystals (grains) by quenching immediately after high-temperature nozzle extrusion during FDM 3D printing. Here, the boundary between the large crystal grains causes the weakening of the binding force. The electrical characteristics of the FDM 3D printing FRS were comparatively analyzed before and after annealing in order to determine the effect of internal stress. The results indicated the presence of structural defects due to molecular orientation, movement of the printing nozzle, and the difference in cooling rate inside and on the surface of the filament after high-temperature extrusion and rapid cooling to room temperature[7].

2.1 Comparison of the electrical characteristics of the 3D printing FRS according to displacement

The TPU is used as a support for the 3D printing FRS. It exhibits elasticity by forming domains within the elastomer where the individual molecules are cross-linked via physical rather than chemical bonding. When an external force is applied that is larger than the physical bond strength, the bond becomes unstable and allows deformation to occur. TPU has a reversible response to an external force such that it returns to its original structure when the external force is removed, and this response can occur repeatedly.

To measure the change in electric resistance according to the displacement of the flexible resistance sensor, the sensor was fixed to the single-axis actuator and 15, 20, and 25% tension was applied, held steady for one second, then allowed to return to the relaxed condition. This procedure was

conducted 10 times and the change in electric resistance was measured via the power line communication (PLC) control. The results presented in Fig. 4 indicate that the maximum value of electric resistance at the peak displacement is not constant during the one-second holding time, but rises and falls in amplitude. For instance, the curve in Fig. 4(a) shows the change in electric resistance and sensor displacement in response to 15% tension. Here, the maximum electric resistance value is obtained at the point of maximum displacement after increasing in direct proportion to the increase in displacement but then decreases during the one-second holding time before subsequently increasing again. Thus, 20 instances of maximum resistance were displayed during the 10 iterations of this test. The instability in the electric resistance value reflected by the change in amplitude during the one-second holding time after maximum displacement was attributed to the difference in resistance stress between the inside and outside of the sensor due to the 3D printing process, as shown in Fig. 5.

The FDM 3D printing FRS is rapidly cooled as soon as it is deposited via the high-temperature extrusion nozzle, so that cooling occurs from the surface of the printing output layer inwards. Hence, the contraction of the surface of the additive layer generates tension in the center in order to maintain the volume, which leads to tensile stress in the surface layer and compressive stress in the center due to resistance against contraction. Since complete cooling in the center takes time, this differential residual stress between the surface layer and the center leads to the change in amplitude with increasing displacement.

Fig. 4(b) shows the change in electric resistance with a 20% increase in displacement. Here, in comparison to Fig. 4(a), the amplitude of the electric resistance is somewhat reduced during the one-second holding time for which the maximum tensile stress is maintained, although the electric resistance pattern exhibits non-uniformity. Furthermore, in the case of

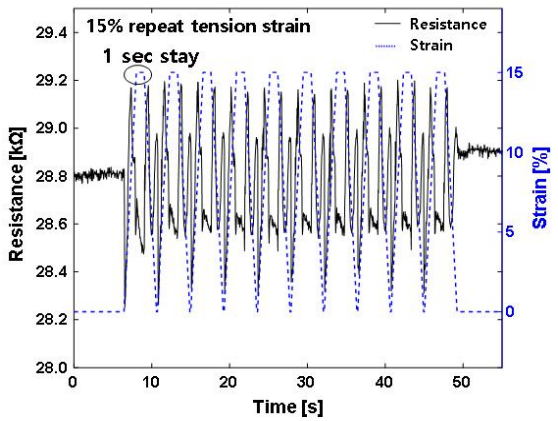

(a) 15% repeat strain-resistance curve

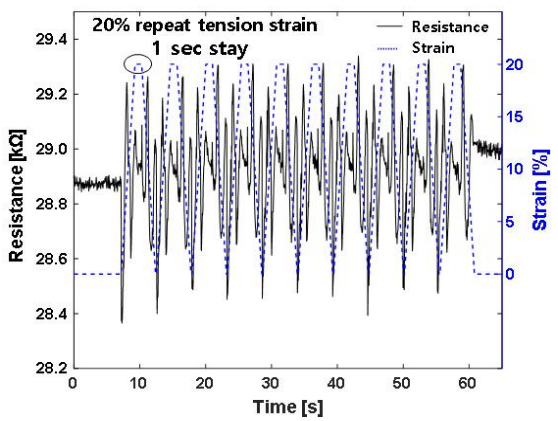

(b) 20% repeat strain-resistance curve

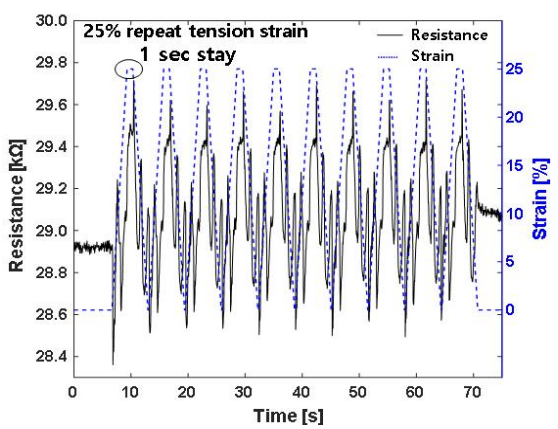

(c) 25% repeat strain-resistance curve

Fig. 4 Strain(blue dashed line)-Resistance(black solid line) curve

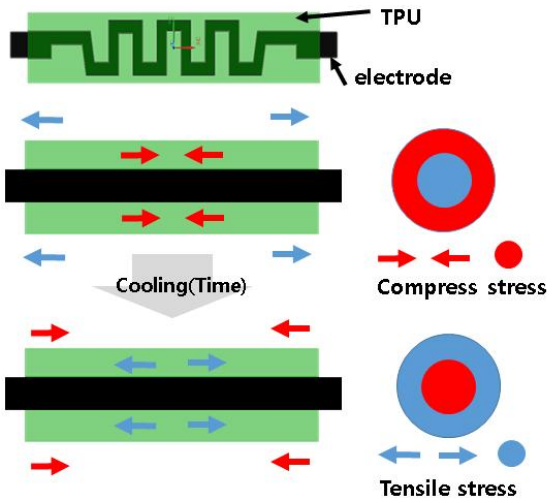

Fig. 5 Simplified schematic drawing of thermally induced residual stress

Fig. 4(c) where the displacement increased by 25%, the amplitude of the electric resistance was further reduced due to the larger external tensile force, the maximum peak values were obtained 10 times, but the displacement curve and electric resistance curves remained mismatched. Moreover, the results in Fig. 4 (a), (b), and (c) all show that the minimum value of the electric resistance was obtained 10 times due to the small repulsive force against the internal residual stress when returning back to the original displacement during maximum displacement.

The experimental results demonstrated that the change in electric resistance of the FDM 3D printing FRS was proportional to the increase in displacement, as indicated by Eq. (1), but this was not matched by the displacement curve. This indicates inadequate performance as a sensor.

$$R = \rho\frac{L}{A},\ \rho = \frac{AR}{L} \quad \cdots\cdots (1)$$

where R : electrical resistance (Ω),
ρ : specific resistance (Ω•mm),
L : specimen length (mm),
A : specimen cross-sectional area(mm^2)

2.2 Comparison of the electrical characteristics of the 3D printed FRS after annealing

In the above section, the inadequate performance of the FDM 3D printed FRS in the measurement of the change in electric resistance with increasing displacement of the sensor was attributed to the generation of structural defects during the printing process, which led to the instability due to residual stress in the printed article. Hence, in the present section, the change in the electric resistance with changing displacement of the sensor was measured using the same process after annealing of the FRS in order to resolve the instability.

Annealing was conducted in the constant temperature oven at the crystallization temperature of the conductive PLA component of the electrode (i.e. 120℃) for two hours followed by cooling to room temperature in the oven.

Fig. 6 presents the results of increasing the displacement by 15, 20, and 25%, holding for one second, then allowing the annealed FRS to return to its initial state. Each test was repeated 10 times. The displacement curve and the change in electric resistance remained well matched to each other and the maximum electric resistance value was maintained even during the one-second holding time at the maximum displacement. In addition, the electric resistance value increased in proportion to the increase in displacement in accordance with Eq. (1).

According to Matthiessen's rule, the influencing factors that affect the electrical conductance are the microstructure and the difference in mobility due to the difference in temperature. Since electrons are scattered by the lattice vibration inside the crystal, the scattering increases as the printing nozzle temperature is raised. In addition, the electrical conductance is affected by microstructural defects such as impurity, precipitation, and dislocation. Thus, the electrical conductance is improved by removing the microstructural defects via annealing.

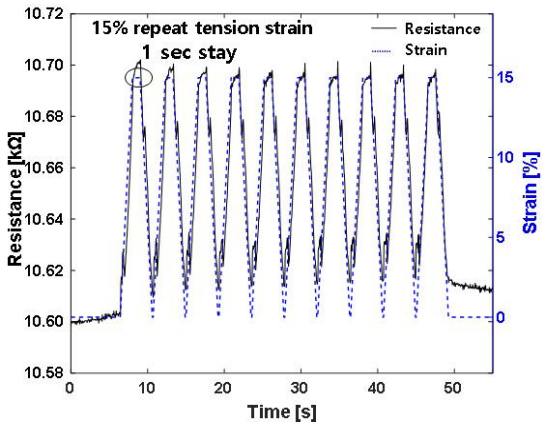

(a) 15% repeat strain-resistance curve after annealing

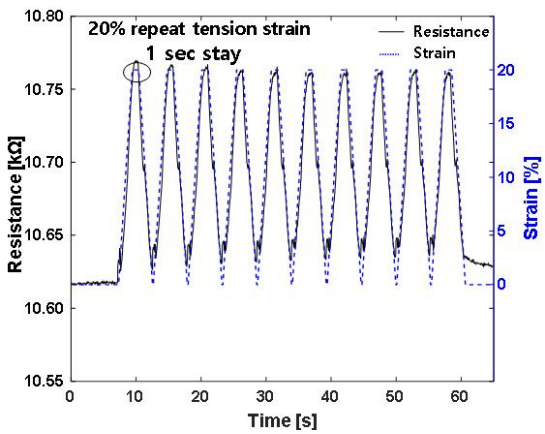

(b) 20% repeat strain-resistance curve after annealing

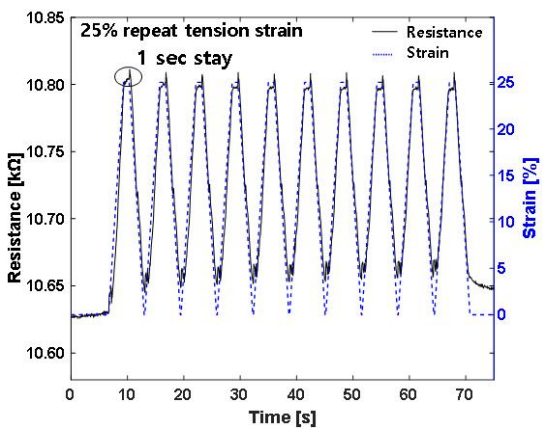

(c) 25% repeat strain-resistance curve after annealing

Fig. 6 Strain(blue dashed line)-Resistance(black solid line) curve after annealing.

The significant improvement in the performance of the 3D printed FRS is thus due to the following reasons: (i) the reduction in vacancies by active atomic diffusion due to the high-temperature annealing process, (ii) improved electrical conductance and stability of the sensor due to removal of unstable energy defects known as dislocations, and (iii) grain coarsening by the maintenance of grain growth due to recrystallization and grain refinement in which the dislocation density is greatly reduced[8-9].

3. Summary

Table 1 presents the electric resistance values according to displacement before and after annealing of the flexible resistance sensor, in which the electric resistance decreased after annealing and increased in proportion to the increasing displacement in accordance with Eq. (1) without any changes in electric resistance due to amplitude variations. This was because the structural defects generated by the FDM 3D printing process were eliminated by annealing.

The residual stress in the FDM 3D printing manufactured article occurs due to the following structural causes: (i) as soon as the molten polymer is deposited by the high-temperature extrusion nozzle during 3D printing, solidification occurs by rapid cooling to room temperature before the polymer chain or filament can become arranged into the

Table 1 3D printing flexible sensor resistance

	Strain [%]	Base resistance [kΩ]	Max. resistance according to amplitude [kΩ]	Resistance at the max. stretch [kΩ]
Before annealing	15	28.81	29.17	28.68
	20	28.88	29.31	29.08
	25	28.91	29.66	29.66
After annealing	10	10.60		10.70
	15	10.63		10.76
	25	10.63		10.81

stable state; (ii) shear strain occurs in the surface of the nozzle wall due to the lower extrusion speed relative to that in the center due to the effect of shear flow caused by friction and cooling during high-temperature extrusion of the 3D printed filament, and (iii) differential stress arises due to polymer orientation, etc.[9-11].

In the present study, meaningful measurements of the change in electrical characteristics were achieved by removing the instability of the 3D printed FRS via the various effects of annealing. This enabled the manufacture of a 3D printed FRS with stable sensing capability. The polymer chain was thus provided with sufficient energy for internal movement and extension, thus reducing the differential residual stress between the inside and outside, increasing the linear elasticity force of the TPU support, and relieving the internal stress due to crystal structure refinement, uniformity, and grain boundary growth, resulting in enhanced reliability and electrical conductance of the polymer electrode.

4. Conclusions

A flexible resistance sensor (FRS) was manufactured using dual 3D printing and its performance was experimentally verified by iterative measurement of the changes in electric resistance with increasing displacement and return to the relaxed state. The structural stability of the printing polymer was found to play an important role in the sensing capability of the 3D printed FRS. Annealing is necessary in order to remove the residual stress due to structural defects arising during the printing process and thus improve the performance and expand the range of application of the sensor. The above results suggest that various flexible sensors with multiple degrees of freedom can be manufactured by a simple FDM 3D printing process without any limitations on size and shape, which will be employed usefully as a major factor in the development of flexible electric devices.

Acknowledgments

This paper was supported by the funding of the project on the development of biomedical technology (NRF-2017M3A 9E2063256) from the National Research Foundation of Korea in the Ministry of Science and ICT, FDM-based multi-material 4D printing and structural design made of Vitremer composite material (Grants No. NRF-2019M3D1A2103919), and Leading Foreign Research Institutes Recruitment Program (GDRC, Inha IST-NASA Deep Space Exploration Joint Research Center), which is a project to develop a Northeast Asia R&D hub in Korea, from the Ministry of Science, ICT and Future Planning.

References

1. Kim, C., Lee, T. K., Kim, T. S., "Measurement Technologies of Mechanical Properties of Polymers used for Flexible and Stretchable Electronic Packaging," Journal of the Microelectronics and Packaging Society, Vol. 23, No. 2, pp 19-28, 2016.
2. Brand, J. van, den., Kok, M, de., Koetse, M., Cauwe, M., Verplancke, R., Bossuyt, F., Jablonski, M., Vanfleteren, J., “Flexible and Stretchable Electronics for Wearable Health Devices,” ELSEVIER, Vol. 113, pp. 116~120, 2015.
3. Choi, J. W., Kim, H. C., "3D Printing Technologies – A Review," Journal of the Korean Society of Manufacturing Process Engineers, Vol. 14, No. 3, pp. 1~8, 2015.
4. Jang, J., Cho, D. W., “A Review of the Fabrication of Soft Structures with Three-dimensional Printing Technology,” Journal of the Korean Society of Manufacturing Process Engineers, Vol. 14, No. 6, pp. 142~148, 2015.

5. Kim, D. B., Lee, G. T., Lee, I. H., Cho, H. Y., “Finite Element Analysis for Fracture Criterion of PolyJet Materials,” Journal of the Korean Society of Manufacturing Process Engineers, Vol. 14, No. 4, pp. 134~139, 2015.
6. Lee, S. K., Kim, Y. R., Kim, S. H., Kim, J. H., “Investigation of the Internal Stress Relaxation in FDM 3D Printing : Annealing Conditions,” Journal of the Korean Society of Manufacturing Process Engineers, Vol. 17, No. 4, pp. 130~136, 2018.
7. Jackson Jr, W. J., & Caldwell, J. R., “Antiplasticization. II. Characteristics of anti-plasticizers,” Journal of Applied Polymer, Vol 11, No. 2, pp 211~226, 1967.
8. Lee, S. K., Kim, Y. R., Park, J. H., Kim, J. H., “Study on Electrical Characteristics of FDM Conductive 3D Printing According to Annealing Conditions,” Journal of the Korean Society of Manufacturing Process Engineers, Vol. 17, No. 6, pp. 55~60, 2018.
9. Hashima, K., Nishitsuji, S., Inoue, T., “Structure − properties of super-tough PLA alloy with excellent heat resistance,” Polymer, Vol. 51, No. 17, pp. 3934-3939, 2010.
10. Postiglione, G., Natale, G., Griffini, G., Levi, M., Turri, S., "Conductive 3D Microstructures by Direct 3D Printing of polymer/carbon Nanotube Nanocomposites via Liquid Deposition Modeling,” ELSEVIER, Vol. 76, pp. 110~114, 2015.
11. Seol, K. S., Shin, B. C., Zhang, S. U., "Fatigue Test of 3D-printed ABS Parts Fabricated by Fused Deposition Modeling," Journal of the Korean Society of Manufacturing Process Engineers, Vol. 17, No. 3, pp. 93~101, 2018.